



Springtime changes in snow chemistry lead to new insights into mercury methylation in the Arctic

Catherine Larose, A. Domergue, Martine de Angelis, Daniel Cossa, Bernard Averty, Nicolas Maruszczak, Nicolas Soumis, Dominique Schneider, Christophe P. Ferrari

► To cite this version:

Catherine Larose, A. Domergue, Martine de Angelis, Daniel Cossa, Bernard Averty, et al.. Springtime changes in snow chemistry lead to new insights into mercury methylation in the Arctic. *Geochimica et Cosmochimica Acta*, 2010, 74 (22), pp.6263-6275. <10.1016/j.gca.2010.08.043>. <insu-00562243>

HAL Id: insu-00562243

<https://insu.hal.science/insu-00562243v1>

Submitted on 11 Mar 2021

HAL is a multi-disciplinary open access archive for the deposit and dissemination of scientific research documents, whether they are published or not. The documents may come from teaching and research institutions in France or abroad, or from public or private research centers.

L'archive ouverte pluridisciplinaire **HAL**, est destinée au dépôt et à la diffusion de documents scientifiques de niveau recherche, publiés ou non, émanant des établissements d'enseignement et de recherche français ou étrangers, des laboratoires publics ou privés.



HAL Authorization

Springtime changes in snow chemistry lead to new insights into mercury methylation in the Arctic

Catherine Larose^{a, b, c}, Aurélien Dommergue^{a, *}, Martine De Angelis^a, Daniel Cossa^d, Bernard Averty^e, Nicolas Maruszczak^a, Nicolas Soumis^a, Dominique Schneider^{b, c} and Christophe Ferrari^a

^a Université Joseph Fourier – Grenoble 1/CNRS, LGGE, 54 rue Molière BP 56, F-38402 Saint Martin d'Hères, France

^b Laboratoire Adaptation et Pathogénie des Microorganismes, Université Joseph Fourier Grenoble 1, BP 170, F-38042 Grenoble Cedex 9, France

^c CNRS UMR 5163, France

^d Ifremer, Centre de Méditerranée, BP 330, F-83507 La Seyne sur mer, France

^e Ifremer, Centre de Nantes, BP 21105, F-44311 Nantes Cedex, France

*: Corresponding author : Aurélien Dommergue, Tel.: +33 0 4 76 82 42 11; fax: +33 0 4 76 82 42 01, email address: dommergue@lgge.obs.ujf-grenoble.fr

Abstract:

Seasonal snow is an active media and an important climate factor that governs nutrient transfer in Arctic ecosystems. Since the snow stores and transforms nutrients and contaminants, it is of crucial importance to gain a better understanding of the dynamics of contaminant cycling within the snowpack and its subsequent release to catchments via meltwater. Over the course of a two-month field study in the spring of 2008, we collected snow and meltwater samples from a seasonal snowpack in Ny-Ålesund, Norway (78°56'N, 11°52'E), which were analyzed for major inorganic ions and some organic acids, as well as total, dissolved, bioavailable mercury (THg, DHg, BioHg, respectively) and monomethylmercury (MMHg) species. We observe a seasonal gradient for ion concentrations, with surface samples becoming less concentrated as the season progressed. A significant negative correlation between BioHg and MMHg was observed in the snowpack. MMHg was positively and significantly correlated to methanesulfonate concentrations. Based on these results, we propose a new model for aerobic methylation of mercury involving species in the dimethylsulfoniopropionate cycle.

1. INTRODUCTION

For High Arctic ecosystems, snow is one of the most important climatic factors. Snow is an active media that transfers particulates and gases between the atmosphere and the landscape (Jones, 1999). It is highly photochemically active with snowpack impurities photolyzed to release reactive trace gases into the boundary layer (Grannas et al., 2007a), and, given its high albedo, fresh snow reflects as much as 90% of incoming radiation (Hinkler et al., 2008). Snow affects both the length of the growing season and primary plant production by acting as a soil insulator as well as a water and nutrient reservoir (Kuhn, 2001; Edwards et al., 2007). Atmospheric scavenging and condensation largely determine snowpack chemistry and snowpacks accumulate particles, solutes and pollutants over winter and spring (Tranter et al., 1986; Loseto et al., 2004). Once deposited, they are subject to redistribution through a variety of processes such as melt-freeze events during the winter season (Johannessen and Henriksen, 1978) and snow metamorphism (Colbeck, 1989; Kuhn, 2001). The geometry of the pore space, vapor pressure gradients and wind pressure, in addition to the physical-chemical properties of the particles themselves can also impact redistribution (Colbeck, 1989; Kuhn, 2001).

The Arctic is exposed to mercury (Hg), a toxic metal that can be transformed to methylmercury (MeHg), a potent neurotoxin that bioaccumulates in food webs (see review by Fitzgerald et al. (2007)), through long-range atmospheric transport. Although there are no direct anthropogenic Hg sources in the Arctic, high levels have been found in the livers and tissues of marine mammals and birds (Wagemann et al., 1998; Campbell et al., 2005) leading to increased exposure for Native Communities that depend on these resources (AMAP, 2009). The discovery of atmospheric mercury depletion events (AMDEs) in the Arctic (Schroeder et al., 1998) led to the hypothesis that these could be the major sources of Hg to Arctic ecosystems. During AMDEs, atmospheric elemental mercury is oxidized to divalent mercury through reactions with halogens such as bromine radicals (Lindberg et al., 2001; Ariya et al., 2002) and then deposited onto snow surfaces at levels 400-800 fold higher than

background in the course of a few hours (Lu et al., 2001; Dommergue et al., 2010). Recent reports suggest that some of this newly deposited Hg is bioavailable, i.e. able to cross biological membranes (Scott, 2001; Lindberg et al., 2002; ~~Larose et al., 2010~~), but its post-depositional fate remains unclear. Field experiments have shown that Hg can be both oxidized and reduced in the snowpack (Lalonde et al., 2002; Dommergue et al., 2003; Poulain et al., 2004) and there is an increasing consensus that most, but not necessarily all, of the deposited mercury is photo-reduced and reemitted back to the atmosphere (Poulain et al., 2004; Kirk et al., 2006; Dommergue et al., 2010).

In addition to the uncertainty regarding Hg sources to the Arctic, the mechanisms that produce MeHg in these cold environments are to date unresolved, although several pathways have been proposed. Methylation can occur both biotically and abiotically; biotic Hg methylation depends on microbial activity and the concentration of bioavailable mercury (BioHg) (Barkay et al., 1997), whereas abiotic methylation depends on the presence of methyl donors. These donors include small organic molecules (i.e. methyl iodide and dimethylsulfide or acetate (Hall et al., 1995; Celo et al., 2006; Hammerschmidt et al., 2007)) and larger organic components of dissolved organic matter such as fulvic and humic acids (Weber, 1993; Siciliano et al., 2005). Hence, the chemistry of the snowpack influences both Hg speciation and its transformation.

Since the snow stores and transforms atmospherically derived pollutants (Colbeck, 1981; Daly and Wania, 2004; Lei et al., 2004), a better understanding of the dynamics of contaminant cycling within the snowpack, and its subsequent release to catchments *via* meltwater would help evaluate ecotoxicological impacts. The timing and magnitude of a pulse exposure is especially important for aquatic ecosystems during spring when biological activity increasingly active (Loseto et al., 2004). The chemical concentrations at the initial stages of melt have been shown to be many times higher (3-7 fold) than averages for the entire snowpack in field and laboratory experiments, a phenomenon referred to as ionic pulse (Johannessen and Henriksen, 1978; Colbeck, 1981; Kuhn, 2001). As the snow begins to melt, soluble ions are removed by the first stages of percolation (e.g. Tranter et al.,

1986), followed by the preferential elution of some ions before others (Eichler et al., 2001). Non-polar organic molecules are also found in meltwater, but are less easily entrained by percolating water due to their low solubility (Meyer et al., 2006). Insoluble particulate material can also be removed by percolation, but usually remains in the snow until the final stages of melting (Hodgkins, 1998; Lyons et al., 2003; Meyer et al., 2006). During spring melt, these soluble and insoluble impurities are released to the environment in a few weeks and can impact the chemistry of snowmelt-fed ecosystems (Williams et al., 2009).

Here, we present chemical data from a seasonal Arctic snowpack sampled over a two-month period in the spring of 2008 in Ny-Ålesund, Norway. The focus of this research is the storage, transfer and subsequent release of solutes and mercury from the snowpack to snowmelt-fed ecosystems. We also explore possible interactions among the different chemical parameters that could potentially be involved in mercury methylation.

2. MATERIAL AND METHODS

2.1 Field site

The spring field study was carried out between April 16th, 2008 and June 8th, 2008 at Ny-Ålesund in the Spitsbergen Island of Svalbard, Norway (78°56'N, 11°52'E). The field site, a 50 m² perimeter with restricted access (to reduce contamination from human sources), is located along the south coast of the Kongsfjorden, which is oriented SE-NW and open to the sea on the west side (Figure 1). The Kongsfjorden was free of sea ice throughout the study.

2.2 Sampling

Surface snow samples were collected daily for Hg speciation. Twice a week, a shallow pit was dug and both surface and basal samples were collected for ion and mercury analyses. Samples for ion measurements were collected in sterile polycarbonate vials (acuvettes®) and stored at -20°C until analysis. For Hg analyses, snow was collected in acid-washed 250 mL glass Schott bottles (see

cleaning protocol outlined in Ferrari et al. (2000) for more details) and subsampled for dissolved and BioHg. Samples for MMHg were collected in 125 mL acid-washed Teflon coated low-density polyethylene bottles, and stored frozen until analysis. The bottles were hermetically sealed, double-wrapped in polyethylene bags, stored at -20°C, and transported frozen to the laboratory. Meltwater was collected in acid-washed 250 mL glass Schott bottles from streams that formed the 1st of June, 2008. In order to determine the spatial variability in mercury deposition, we sampled two snowpits integrating snow fall since the previous summer, the first on the Høltedahlfonna glacier (sample date 30/04/08, N79°08.17, E13°16.12, 1173 m asl, 40 km from the Kongsfjorden fjord) and the second on the Kongsvegen glacier (sample date 19/05/08, N78°45.29, E13°20.20, 670 m asl, 40 km from the Kongsfjorden) (Figure 1). The Høltedahlfonna pit, with a depth of 1.80 m, was sampled at 20 cm intervals, whereas the Kongsvegen pit, with a depth of 2.75 m, was sampled at 30 cm intervals. Field blanks were collected, filled with ultrapure water in the laboratory, opened during sample collection, and handled as samples. To avoid contamination, Tyvex® body suits and latex gloves were worn during sampling and gloves were worn during all subsequent handling of samples.

2.3 Chemical analyses

2.3.1. Total Hg & speciation

Total Hg (THg) in snow samples was measured in the field with a Tekran model 2600 using USEPA method 1631 revision E. Samples were oxidized with 0.5% v/v BrCl to preserve divalent Hg (Hg(II)) in solution and to digest strongly bound Hg(II) complexes. Excess BrCl was neutralized with pre-purified hydroxylamine hydrochloride. The sample was then automatically injected, together with SnCl₂, into a reaction vessel, reducing Hg(II) to gaseous elemental Hg (Hg⁰). Hg⁰ was carried in an argon stream to two online gold traps. After thermal desorption, Hg⁰ was detected by atomic fluorescence spectrometry. The Tekran Model 2600 was calibrated every day with the NIST SRM-3133 Hg

standard. The limit of detection, calculated as 10 times the standard deviation of a set of 10 blanks, was 0.3 ng.L^{-1} and relative accuracy was determined as $\pm 8\%$ using a certified reference material (ORMS-4, National Research Council Canada). All samples were analyzed in triplicate. Dissolved total Hg (DHg) concentrations were determined in all samples by measuring Hg concentrations after filtration on a $0.45 \text{ }\mu\text{m}$ nylon filter (25 mm diameter, Cole-Parmer). Bioavailable Hg (BioHg) concentrations were determined using ~~the biosensor described in Larose et al. (2010).~~ BioHg is defined as the fraction of Hg able to enter cells. BioHg is detected using a genetically modified bacterium containing mercury resistance and luminescence genes, such that photons are produced in a dose dependent manner upon Hg exposure. Briefly, the biosensor was cultured overnight in LB medium containing $100 \text{ }\mu\text{g.mL}^{-1}$ ampicillin at 37°C without agitation. The culture was resuspended in LB media and experiments were carried out using cells in mid-exponential growth phase (OD_{600} of 0.4). Cells were exposed to either a series of Hg dilutions in order to obtain a standard curve, or to melted snow samples with unknown bioavailable Hg concentrations in a v/v ratio (sample volume added is equal to the volume of the biosensor solution) and incubated for two hours at 37°C without agitation. The Hg standards were prepared from serial dilutions of a Hg^{2+} solution (SRM-3133 Hg standard). Samples were analyzed in triplicate, with three independent cultures, and light emission was recorded using a Modulus luminometer. Luminescence was expressed as relative light units (RLU) and normalized for optical density.

2.3.2. Monomethylmercury analysis

MMHg was measured on unfiltered samples as volatile methyl mercury hydride, by purge and cryo-trapping gas chromatography, and detected as elemental Hg vapor by atomic fluorescence spectrometry (Tekran, Model 2500). The mercury hydrides (from methyl and inorganic mercury) were synthesized in the presence of NaBH_4 , purged from the sample with He, concentrated and then separated by cryogenic chromatography before being converted into Hg^0 in a furnace (800°C) and

detected by the AFS detector. This protocol is derived from the hydride generation technique described by Tseng et al. (1998) and improved by Stoichev et al. (2004). The hydrides are formed within a glass reactor and the column used is a silanized glass tube filled with Chromosorb W/AW-DMCS impregnated with 15% OV-3. Analytical reproducibility varied with time between 6% and 15%. Calibration was performed using dilutions of a 1 g.L^{-1} stock MMHg solution in isopropanol into an aqueous HCl (0.4% Suprapur, Merck) solution. In addition, we used certified reference material, the ERM-AE670 from the Institute for Reference Materials and Measurements (IRMM, European Commission), which is $\text{CH}_3^{202}\text{HgCl}$ in a 2 % ethanol/water solution. The recovery of 0.05 and 0.1 pmol.L^{-1} of ERM-AE670 spikes in seawater samples was $103 \pm 2\%$ and $99 \pm 2\%$, respectively. The MMHg measurements took place within two months of sampling.

In order to determine Hg speciation within the snowpack, Vinteq simulations (Visual MINTEQ), that include parameters such as chemical equilibrium, major ions, pH and some short chain organic compounds, were carried out.

2.3.3. Additional analysis

The pH of melted snow samples was measured at 20°C (Heito pH meter, Paris). The electrode was manually calibrated, prior to analysis, with three different pH buffers (pH 4, 7 and 10, Heito). The values were not corrected for *in situ* snow temperature. In order to examine possible interactions between Hg speciation and snow chemical composition, inorganic ions (F^- denoted FI, NO_3^- , Cl^- , SO_4^{2-} , NH_4^+ , Ca^{2+} , Na^+ , K^+ and Mg^{2+}) and organic acid (methylsulfonic acid (MSA), glutaric acid (Glut), oxalic acid (Ox), acetate with a possible contribution of glycolate (Ace.Glyc), and formate) concentrations were measured at the Laboratoire de Glaciologie et Géophysique de l'Environnement by conductivity-suppressed Ion Chromatography using a Dionex ICS 3000. Due to the proximity of the fjord, leading to very high chloride and sodium concentrations, samples were diluted 10-fold for organic acids and minor ions and 100-1000 times for major ions prior to analysis.

2.4 Statistics

All data, with the exception of pH values, were log-transformed prior to statistical analysis in order to obtain data with a normal distribution. The transformation was successful for all data. Statistical data analysis was performed using JMP 5.1 software (SAS Institute, 2003) and R (The R Project for Statistical Computing <http://www.r-project.org>). Simple linear regression analysis was carried out to detect associations between the different chemicals. Principal component analysis (PCA) was performed to reduce the dimensionality of the data set using the ade4 data package for R. Samples were clustered using Ward's linkage for hierarchical cluster analysis, where the error sum of squares at each successive clustering step is minimized. Analysis of variance (ANOVA) and Tukey-Kramer HSD multiple comparison tests were then used to determine significant differences in chemical parameters among the different clusters in JMP 5.1. Statistical significance was set at a probability level $\alpha < 0.05$.

3. RESULTS

3.1 Snowpack dynamics

The seasonal snowpack began to develop in October, 2007, but a rain event in January 2008 resulted in a decrease in snow depth and the formation of a relatively thick (~10 cm) ice layer above the soil surface. The snowpack reformed above the ice layer, had a thickness of about 40 cm at the beginning of the sampling period (16th of April), but had disappeared almost completely by the 8th of June. Snow melt began mid-May (around the 20th) and meltwater rivers that flowed to the fjord formed on the 1st of June, 2008. A total of 7 snowfall events occurred throughout the field season.

3.2 Snowpack and meltwater chemistry

The snowpack is strongly influenced by marine aerosols due to the proximity of the fjord, although continental sources possibly contribute to Na⁺ and Mg²⁺ concentrations. The dominant cations in the

snowpack were Na^+ ($1861 \mu\text{mol.L}^{-1}$) followed by Mg^{2+} ($426 \mu\text{mol.L}^{-1}$) and Ca^{2+} ($110 \mu\text{mol.L}^{-1}$), while the dominant anions were Cl^- ($2119 \mu\text{mol.L}^{-1}$) followed by SO_4^{2-} ($159 \mu\text{mol.L}^{-1}$) and NO_3^- ($5 \mu\text{mol.L}^{-1}$). In meltwater, the average concentrations for cations and anions were 433, 263 and $359 \mu\text{mol.L}^{-1}$ for Na^+ , Mg^{2+} , Ca^{2+} , respectively, and $569 \mu\text{mol.L}^{-1}$ for Cl^- , $90 \mu\text{mol.L}^{-1}$ for SO_4^{2-} and $4 \mu\text{mol.L}^{-1}$ for NO_3^- (Entire data ranges are given in Supplementary material Table I). In the snowpack, pH ranged from acidic to circumneutral values (4 to 6.6) and was stable at a pH around 6.8 in meltwater.

Based on the Vimteq results, mercury chloride (HgCl_2) is the dominant form of Hg complexes in all our samples, followed by HgBrCl , HgCl_3^- , HgBr_2 . The speciation of Hg is driven by the large chloride concentrations, but remains uncertain due to the lack of knowledge on binding constants of mercury with organic matter and the lack of robust speciation data of organic matter in snow. The presence of Hg complexes bound to organic compounds could readily change the photoreactivity and bioavailability of these complexes.

We performed PCA analysis and then clustered the samples using Ward's linkage. The clustering results are presented in Table I and the PCA is presented in Figure 2. Seasonality is apparent, since Group 1 comprises early season surface samples and most of the basal samples, Group 2 contains mid-season surface samples, Group 3 contains late-season surface samples, and Group 4 is composed of meltwater samples. Although precipitation events occurred at different times throughout the field season, they had no effect on sample distribution within the PCA, since samples collected during snowfall events did not cluster together. In the graphical representation of the PCA analysis, the length of the arrow represents the relative importance of the associated parameter in determining the distribution of samples. Based on the PCA analysis carried out on our data, the most important parameters driving sample distribution are BioHg and THg (Group 1), MMHg, MSA and Glut (Group 2), inorganic ions (Group 5) and certain organic acids (Group 4). The clustering of samples in Group 3 is driven by low concentrations of inorganic ions and organic acids.

ANOVA and multiple comparison tests were carried out in order to determine significant differences in chemical parameters among the five groups derived through PCA analysis and clustering using Ward's linkage. The results of these comparisons are presented in Table I (Supplementary material). Chemical parameters varied significantly among groups, with the exception of THg, DHg and BioHg (data not shown) (Table I, Supplementary material). There appears to be a seasonal gradient, with early season snow (Group 1) that is generally more concentrated than snow sampled later in the season (Groups 2 and 3). Meltwater (Group 4) is enriched in ions relative to snow, with the exception of the five snow samples in Group 5 that had the highest mean Na^+ , NH_4^+ , K^+ , Mg^{2+} , Cl^- , SO_4^{2-} and Br^- concentrations. Group 5 and Group 4 had the highest Ca^{2+} concentrations, and Group 4 had the highest levels of NO_2^- and organics.

Group 2 had the highest NO_3^- concentrations and Groups 2 and 4 had the highest MSA and glutaric acid levels. MSA and glutaric acid levels peaked in surface samples during May (Figure 3) and are significantly and positively correlated ($r^2=0.62$, $p=0.0013$, $n=13$). There are no significant differences among the groups in terms of Na:Cl and Br:Cl ratios, and the mean values of these ratios are close to those of seawater (Na:Cl=0.855 and Br:Cl=0.0015). The meltwater group has significantly higher K:Cl and Mg:Cl ratios (0.052 and 0.474, respectively) than the other groups, for which the ratios are similar to seawater (K:Cl=0.0186 and Mg:Cl=0.193). Group 5 had the lowest Ca:Cl ratio, which is close to the seawater ratio (0.044), while the other groups had significantly higher values. The SO_4 :Cl ratio was highest in Group 2 at 0.430, and was closest to the seawater ratio (0.103) in Groups 5 and 1.

Meltwater samples were collected as of the 1st of June. The first sample collected had the highest Na^+ , Cl^- , K^+ , Mg^{2+} , SO_4^{2-} and MSA concentrations (Figure 4) and appears to correspond to the tail-end of the ionic pulse. Glutaric acid, NO_3^- and NO_2^- concentrations increased as melting progressed and no peak in Br^- and NH_4^+ concentrations was observed. MMHg concentrations were highest in the first meltwater sample (1st of June), whereas concentrations of BioHg, DHg and THg peaked on the 2nd, 6th and 7th of June, respectively (Figure 4).

3.3 Hg dynamics

At the onset of sampling (April 16th, 2008), surface snow had high THg concentrations, with levels reaching almost 90 ng.L⁻¹. These concentrations dropped to around 1 or 2 ng.L⁻¹ by the 9th of May and increased again just prior to melt. THg concentrations in basal snow were relatively low at the beginning of the sampling period and increased gradually to levels above those of the surface around the 9th of May. THg concentrations in both basal and surface snow increased slightly from the 17th to the 23rd of May (Figure 3). BioHg concentrations were higher in surface samples than basal samples and peaked at the beginning and end of the sampling period (Figure 3). No MMHg data for surface samples was available between April 16th and May 6th since THg concentrations were too elevated to allow the detection of the MMHg peak with our analytical setup, but as of May 9th, concentrations were around 0.045 ng.L⁻¹ and dropped progressively to about 0.010 ng.L⁻¹ by May 25th. Two large MMHg peaks were measured in surface snow on the 21th and 27th of May with concentrations reaching 0.299 and 0.511 ng.L⁻¹, respectively. Basal snow MMHg levels were measured throughout the field period and concentrations were low, averaging 0.010 ng.L⁻¹, with the exception of a peak (0.245 ng.L⁻¹) on the 2nd of June (Figure 3).

Linear regression analysis was carried out to explore the relationship between different Hg species and the major parameters influencing sample distribution as determined by PCA analysis. No significant linear correlations were obtained between MMHg and SO₄²⁻, NO₃⁻ or Cl⁻ concentrations when samples were analyzed either together, by group or based on sampling depth. THg concentrations were correlated to Cl⁻ concentrations in surface samples ($r^2=0.31$, $p=0.0032$, $n=26$) and basal samples ($r^2=0.31$, $p=0.039$, $n=14$). Based on PCA analysis, MMHg and MSA concentrations are correlated, and both are anti-correlated to BioHg concentrations. MSA, MMHg and glutaric acid also appear to be correlated (Figure 2). Linear regression analysis was carried out to determine the significance of these relationships and MMHg and MSA are significantly, positively correlated ($r^2=0.45$, $p=0.0022$, $n=18$), as are Glut and MSA ($r^2=0.62$, $p=0.0013$, $n=13$), but there is no significant

linear relationship between MMHg and Glut ($r^2=0.02$, $p=0.70$, $n=9$). MMHg and BioHg are significantly, negatively correlated in the snowpack ($r^2=0.26$, $p=0.0044$, $n=26$), as are BioHg and MSA ($r^2=0.52$, $p=0.0018$, $n=15$), while no significant relationship exists between BioHg and Glut ($r^2=0.08$, $p=0.47$, $n=8$).

THg and MMHg concentrations in glacier snowpits are presented in Figure 5. THg in both pits decreased rapidly with depth, with buried layers showing low or undetectable values. Both pits exhibit similar MMHg patterns with the highest concentrations at the surface, decreasing over the first 50 cm, then increasing to a peak at ~150 cm, and decreasing below. In the Kongsvegen pit (Figure 5), unlike the Holtedahlfonna pit, MMHg levels increased again in the lowest part of the pit. Organics (MSA, glutaric acid) could only be detected in surface and bottom layers while $\text{SO}_4\text{:Cl}$, Na:Cl and Br:Cl ratios were similar to seawater. Mg:Cl , K:Cl and Ca:Cl ratios were much higher than those of seawater. The detailed chemistry for both pits is given in Table II. No significant correlations were observed between MMHg and Hg, or between Hg species and ion concentrations.

4. DISCUSSION

4.1 Snowpack and meltwater chemical composition

The snowpack evolves chemically over time. We observe a seasonal gradient in ion concentrations in the snowpack, with the highest concentrations for most ions observed in early season surface and basal snow (Group 1), whereas the lowest concentrations were observed in samples collected in late spring, just prior to melt (Group 3). Melting can occur at air temperatures below 0°C when solar radiation is sufficiently intense and penetrates into the snowpack (Kuhn, 1987). As a result, the top snow layers melt first and the surface layers gradually become less concentrated in ions and particles as the season progresses. The photochemical reactivity of surface layers also contributes to changes in ion concentrations, with snowpack impurities photolyzed to release reactive trace gases such as

NO₂, HONO, CH₂O, BrO and Hg⁰ to the boundary layer. These processes appear to be ubiquitous and their influence varies according to background radical concentrations (Grannas et al., 2007b).

Our results are consistent with those of Goto-Azuma et al. (1994) who observe higher ion concentrations at the base of an Arctic snowpack as a result of percolation and snowpack metamorphism. The surface and basal samples in Group 5 had the highest ion concentrations among all groups, including the meltwater group. This is surprising since meltwater mobilizes solutes and contaminants within the snowpack, thus becoming enriched relative to the snow (Kuhn, 2001; Meyer and Wania, 2008). The samples in Group 5 carry a strong marine salt signal, as determined by the different ion to Cl⁻ ratios (Table I, Supplementary material). It is likely that the surface sample of this group (sample date 19/04/2009) contained sea-spray and was enriched by marine air masses. The signal of this event can later be traced in the basal samples following snowfall and elution. It is also possible that the highly concentrated basal samples consist of older snow that had undergone similar deposition events from marine air masses.

Mid-season surface snow samples (Group 2, May 9th to May 30th) had high levels of glutaric acid, MSA and NO₃⁻, in addition to the highest SO₄²⁻ to Cl⁻ ratio among all groups. Glutaric acid, a C₅ dicarboxylic acid commonly found in aerosols and as cloud-condensation nuclei, is derived from a variety of sources including anthropogenic emissions such as motor exhaust, as well as biogenic emissions from the ocean (Kawamura and Ikushima, 1993; Kawamura and Kasukabe, 1996). Senescent marine phytoplankton cells release lipidic cell components (chlorophyll, chlorophyll phytyl chain, carotenoids, sterols, and unsaturated fatty acids (oleic acid, alkenones and unsaturated alkenes) (Rontani, 2001) that can be photooxidized to shorter diacids. Among the diacids, oxalic acid is generally the most abundant in aerosols, followed by succinic, malonic and glutaric acid (Kawamura and Kasukabe, 1996). This has been observed in diverse environments worldwide, including the Arctic. Another pathway involved in diacid production is the reaction of O₃ with cyclohexene, a symmetrical alkene molecule (Rontani, 2001). Hence, diacids in the marine environment originate

from two major processes: long-range transport from industrialized continents and *in situ* photochemical production. Legrand et al. (2007) reported seasonal differences in diacid concentrations in aerosols of a coastal site, with high oxalic acid and low C₅ and C₄ concentrations in the winter. They proposed that ageing of air masses during transport favored the production of short-chain diacids through the successive oxidation of C₅ and C₄ diacids. This is consistent with our data, as the early season snow oxalic acid in the first sample of Group 5 seems to originate from older marine air masses that travelled over the Arctic Ocean (HYSPLIT air mass trajectory model, data not shown). Glutaric acid was almost undetectable at the beginning of the season, but concentrations were high in samples from Group 2 collected in surface snow during the month of May. In the summer, Legrand et al. (2007) reported peak concentrations of C₅ and C₄ acids in a mid-latitude marine atmosphere, which may be attributed to unsaturated fatty acid degradation. The high glutaric acid concentrations relative to oxalic acid in our data set suggest that fatty acids originated from proximal marine emissions as the succession of oxidations to shorter diacids did not lead to total C₅ and C₄ depletion. Glutaric acid is also significantly positively correlated to MSA, which further supports the presence of a close marine source of organic acids. MSA is a photo-oxidation product of DMS, which itself is a derivative of dimethylsulphoniopropionate (DMSP) produced by phytoplankton (Bentley and Chasteen, 2004). DMSP is known as both an osmoprotectant and cryoprotectant for microorganisms, as well as a carbon and sulfur source. It is released from senescent or stressed cells (Kiene et al., 2000). MSA has been shown to exhibit a distinct seasonality that is linked to biological activity in Arctic waters and the importance of the phytoplankton bloom to dimethylsulfate (DMS) concentrations has also been reported (Leck and Persson, 1996). The most recent published data available on algae blooms in Svalbard were collected in 2007 and show that the bloom occurred in May (Narcy et al., 2009). Although the data for the 2008 period are unavailable, it is likely that the bloom occurred at the same period of the year.

The chemical changes of a snowpack and runoff are influenced by the chemical composition of the snow and wintertime refreezing processes of the meltwater (Colbeck, 1981; Davies et al., 1982; Bales et al., 1993). The first flush of meltwater is usually highly concentrated, with the preferential elution of certain solutes over others leading to a pulse (Colbeck, 1981; Goto-Azuma et al., 1994). Meltwater samples had mean ion concentrations that were comparable to those reported for early seasonal snow (Group 1), with the exception of K^+ , Mg^{2+} and Ca^{2+} concentrations, which were much higher. In addition, the Mg:Cl, K:Cl and Ca:Cl were also significantly higher than in the early season samples. These elevated ratios may reflect the contact between the meltwater and the soil, since meltwater can be modified by soil processes due to infiltration and leaching (Williams et al., 2009) in addition to the flushing of soil pore fluids upon soil thaw. Although solute concentrations in the first meltwater sample are high, it is likely that the pulse occurred before the formation of meltwater rivers and that we only measured the tail-end of the pulse, since we were unable to detect preferential elution. Nevertheless, we did observe some fractionation of mercury species, as MMHg was preferentially eluted to BioHg, followed by the dissolved fraction. The chemical composition of the DHg fraction is unknown, but likely consists of different forms of Hg that are soluble, but not bioavailable. The remaining Hg was eluted last and was probably bound to insoluble particles (Figure 4).

4.2 Snowpack Hg dynamics

While AMDEs have been shown to lead to high deposition of Hg onto snow surfaces, the post-depositional fate of Hg has yet to be completely clarified. The current consensus among researchers now is that a large portion is reemitted back to the atmosphere following an event (Poulain et al., 2004; Kirk et al., 2006; Dommergue et al., 2010). We recorded an AMDE at the beginning of the field season that led to high concentrations in the snowpack (max value 90 ng.L^{-1}), but these decreased rapidly. At the beginning of the field season, basal snow sample Hg concentrations were low, around $1\text{-}2 \text{ ng.L}^{-1}$, yet they increased almost 8-fold following the AMDE-induced peak in surface snow

concentrations. Although the transfer mechanisms that lead to this increase are unclear, Hg was likely transferred into deeper layers of the snowpack from the surface bound to particulate matter or as a mobile chemical form that percolated through the snowpack (Daly and Wania, 2004; Johnson et al., 2008). If the Hg levels in the basal layers of the snow result from AMDEs, then the quantity retained by the snowpack represents roughly 10% of the initial loading. These results suggest that although a large portion of Hg deposited by AMDEs returns to the atmosphere, a significant quantity is trapped within the snowpack, from which it can then be transferred to other systems upon melting.

In a review on Hg microbiogeochemistry in polar environments, Barkay and Poulain (2007) outline possible methylmercury sources and methylation pathways in arctic ecosystems. These include atmospheric and aquatic sources with either abiotic or biotic methylation pathways. In terms of snowpack MMHg concentrations, the most plausible sources are: 1) an atmospheric source of MMHg due to the photodegradation and deposition of plankton-derived dimethylmercury, 2) *in situ* methylation of BioHg in the snowpack (microbial), 3) biotic or abiotic methylation in the atmosphere, and 4) *in situ* phytoplankton MMHg production.

Based on a positive correlation between MMHg and chloride in snow collected from Ellesmere Island, Nunavut, Canada, St. Louis et al. (2005) suggested that MMHg was bound to seasalt aerosols (i.e. source 1). Constant et al. (2007) also reported a similar correlation in subarctic snow. This led to the hypothesis that MMHg originated from gaseous dimethylmercury (DMHg) formed by phytoplankton in the water column, whose production has been reported in Arctic waters (Kirk et al., 2008). Since DMHg is highly volatile, it can be emitted from the seawater and be oxidized to MMHg in the atmosphere by free radical species such as OH^\bullet and Cl^\bullet (Niki et al., 1983a; Niki et al., 1983b) before being deposited onto nearby snow surfaces (St. Louis et al., 2005). However, no correlation between MMHg and chloride was observed in our data set, even when the different snow types and groups are analyzed individually. St Louis et al. (2007) also observed a lack of correlation between MMHg

and chloride, but still attributed MMHg concentrations to DMHg production and subsequent photodegradation based on the proximity of their sampling sites to the water.

MMHg is significantly anti-correlated to BioHg in our snow samples, which could suggest that a fraction of the BioHg is efficiently scavenged to form MMHg. Bacteria have been isolated from Arctic snowpacks (Amato et al., 2007) and microbial activity has been measured at temperatures down to -20°C (Christner, 2002). Poulain et al. (2007) reported the presence of Hg resistance (*merA*) gene transcripts in Arctic biofilm samples and, hence, it is likely that the microbial populations in Arctic environments are able to metabolize mercury. Whether Hg methylation can occur in the snow remains uncertain. Constant et al. (2007) reported increases in the MMHg:THg ratio that were positively correlated with bacterial colony counts and particles. These results led to the hypothesis that MMHg was being formed within the snowpack, despite the absence of correlation with sulfate-reducing bacteria (SRB), the principal methylators in anoxic environments. Since the snowpack is most likely oxygenated, other species capable of methylating Hg aerobically may exist.

Hg methylation has been linked to sulfur and iron metabolism in bacteria (Fleming et al., 2006; Kerin et al., 2006). Early research into the mechanisms of Hg methylation was based on anoxic sediments (Compeau and Bartha, 1985; Berman et al., 1990) and quickly focused on anaerobic, sulfate reducing bacteria. Choi et al. (1994) used radio-labeled ¹⁴C incorporation and enzyme activity measurements to propose that methylation involves the tetrahydrofolate (THF) pathway in *Desulfovibrio desulfuricans*. In their model, the methyl group is transferred from CH₃-tetrahydrofolate via methylcobalamin with either serine or formate as the original methyl donors during the acetyl-CoA synthase pathway.

In our samples, MMHg is positively correlated to MSA, a by-product of DMSP and an important molecule in the marine microbial sulfur cycle (Kiene et al., 2000). DMSP can be metabolized *via* several different pathways in the water column (Figure 6), one involving enzymatic cleavage to produce DMS, but also by demethylation and demethiolation to produce methylsulfate in bacterial

cells. Methylsulfate can then undergo thiol transmethylation to produce DMS (Bentley and Chasteen, 2004). The initial demethylation (and a possible second demethylation) has recently been shown to be THF-dependent and catalyzed by an amino-methyltransferase enzyme in aerobic bacteria (Reisch et al., 2008). The similarities to anaerobic Hg methylation are striking, and it is possible that a fraction of BioHg, upon entering the cell, undergoes methylation by aerobic bacteria that are able to demethylate or metabolize DMSP. A total of four methyl transfer reactions occur at various stages of DMSP metabolism, and BioHg may serve as a methyl group acceptor at some point in the process. BioHg is also negatively correlated to MSA, which further suggests DMSP implication (or the implication of another product of DMSP metabolism) in the methylation of Hg. This is compounded by the fact that neither MMHg nor BioHg concentrations are significantly correlated to glutaric acid, a biogenically produced dicarboxylic acid. Finally, this hypothesis is reinforced by recent results demonstrating Hg methylation in the oxic oceanic water column (Monperrus et al., 2007; Cossa et al., 2009; Sunderland et al., 2009).

Whether methylation occurs within the snowpack, in the water column or both simultaneously remains under debate, but, methylation appears to require a substrate involved in DMSP cycling. Hence, coastal sites may be especially at risk for MMHg contamination, since they are reported to contain higher Hg concentrations than inland sites (Douglas and Sturm, 2004; Brooks et al., 2008) and are close to a DMSP source. In addition, the run-off during springtime melt may return concentrated water back to the aquatic ecosystem.

Although the case for biologically-produced MMHg is strong, the data from the snow pits sampled on April 30th and May 19th point to a combination of sources for MMHg in remote areas. Since the fjord is 40 km away from both sampling sites, its effect on the chemical composition of snow is less important, as reflected by the 1-3 order of magnitude lower Na⁺ and Cl⁻ concentrations measured in our pit samples. MMHg concentrations were generally higher than in the surface waters of the fjord (seasonal average 10 ± 4 pg.L⁻¹) and higher than average MMHg levels in the seasonal snowpack,

excluding the peaks measured towards the end of May. In addition, BioHg and MSA concentrations were generally below detection limit in these samples, which would exclude the biotic methylation mechanism outlined above. THg levels were also low, and neither THg nor MMHg were significantly correlated to Cl^- concentrations. Taken together, these results suggest alternate sources for MMHg. Abiotic methylation may be occurring in the atmosphere and involve methyl donors such acetate and reactive mercury (not strongly bound) in the aqueous phase, as proposed by Hammerschmidt et al. (2007). Methylation kinetics obtained by Gardfeldt et al. (2003) suggest a reaction pathway where Hg(II) is bound to organic complexes. Nevertheless, this does not exclude an oceanic source for MMHg, since the layers with marine organics also exhibit the highest MMHg concentrations. Finally, the elevated levels of MMHg in the Kongsvegen basal layer may point to biotic methylation. Amato et al. (2007) found higher concentrations of bacteria in the summer layer in a pit dug on the same glacier and this may reflect microbial growth and metabolism. These potential sources of MMHg may have been masked at the coastal site by the influence of the fjord. It is likely that MMHg is supplied to Arctic environments by various pathways that are occurring simultaneously.

Acknowledgements

This work is funded by EC2CO, LEFE-CHAT and by the French Polar Institute IPEV for logistical support (program CHIMERPOL). We acknowledge Alan Le Tressoler and AWIPEV for field support, as well as Emmanuel Prestat for advice on statistics and I. Moreno and J. Cozic for their help in the laboratory. We would also like to thank M. Legrand for the scientific discussions. CL would like to acknowledge the FQRNT (le Fond Québécois de la Recherche sur la Nature et les Technologies) for a PhD research fellowship.

471

472 Table I: Groups, corresponding samples and sample dates as derived by PCA analysis and Ward's
473 linkage for hierarchical clustering analysis

Cluster name	Nature of the sample	date	474
Group 1	Early season surface snow and most of basal snow samples	16/04/08 to 06/05/2008	475 476
Group 2	Mid-season surface snow	09/05/2008 to 30/05/2008	477
Group 3	Late-season surface snow	01/06/2008 to 8/06/2008	
Group 4	Meltwater samples	01/06/2008 to 08/06/2008	478
Group 5	An early surface sample and four basal samples	19/04/2008, 23/04/2008, 29/04/2008, 09/05/2008, 20/05/2008	479 480

481

482

483

484

485 Table II: Measured species concentrations at different depths at the Holtedahlfonna (H) and
 486 Kongsvegen (K) snowpits. Ion concentrations are expressed in $\mu\text{mol.L}^{-1}$. Standard error was less than
 487 10%.

488

Snow sample	MSA	Cl ⁻	Br ⁻	NO ₃ ⁻	Glut	SO ₄ ²⁻	Na ⁺	NH ₄ ⁺	K ⁺	Mg ⁺⁺	Ca ⁺⁺
H 0cm	0.12	5.6	0.00	1.3	0.03	5.4	5.4	1.6	0.13	1.8	1.8
H 20 cm	0.00	18.1	0.22	0.6	0.00	1.8	17.3	0.6	0.19	3.9	1.8
H 40 cm	0.00	62.4	0.52	3.1	0.00	8.4	56.8	2.2	0.89	16.3	4.8
H 60 cm	0.00	35.8	0.43	0.8	0.00	3.5	32.9	1.2	0.38	11.3	3.8
H 80 cm	0.00	46.2	0.43	0.7	0.00	4.7	37.8	1.1	0.37	12.6	2.7
H 100 cm	0.00	7.3	0.09	0.5	0.00	1.9	6.5	0.7	0.08	2.5	1.7
H 120 cm	0.00	22.0	0.22	0.7	0.00	2.1	19.4	1.3	0.29	6.4	1.9
H 140 cm	0.00	14.6	0.13	0.4	0.00	1.5	14.0	0.4	0.15	4.3	1.4
H 160 cm	0.00	0.9	0.00	0.4	0.00	0.6	0.8	0.5	0.03	0.3	0.9
H 180 cm	0.12	3.7	0.00	1.6	0.00	2.3	0.8	0.8	0.09	4.1	3.8
K 0 cm	1.66	13.5	0.22	3.1	0.07	16.1	12.0	4.7	0.11	5.9	4.7
K 30 cm	0.00	15.1	0.22	0.6	0.01	2.6	13.7	0.6	0.15	5.2	1.9
K 60 cm	0.00	39.0	0.30	2.0	0.00	5.7	38.4	1.0	0.35	11.7	3.3
K 90 cm	0.00	100.4	0.90	1.0	0.00	10.8	85.7	1.0	1.37	28.1	6.4
K 120 cm	0.00	34.2	0.34	1.1	0.00	3.2	34.7	0.4	0.40	10.3	2.1
K 150 cm	0.00	21.3	0.22	0.9	0.00	4.4	19.9	1.0	0.26	6.7	2.5
K 180 cm	0.00	46.4	0.47	0.5	0.00	5.3	40.5	1.3	0.45	17.0	3.3
K 210 cm	0.00	25.9	0.30	0.9	0.01	3.6	25.5	1.2	0.35	9.1	4.6
K 240 cm	0.10	12.0	0.13	0.5	0.03	3.6	12.2	0.9	0.17	5.7	3.3
K 270 cm	0.02	6.9	0.13	0.1	0.00	0.4	5.4	0.5	0.10	1.3	0.6

489

490

491

FIGURE CAPTION

Figure 1: Map of the study area. Left map: Location of the Svalbard Archipelago. Right map: Ny-Ålesund (black star), Svalbard (Norway) and its surroundings. Sampling sites on the glaciers are shown with black triangles.

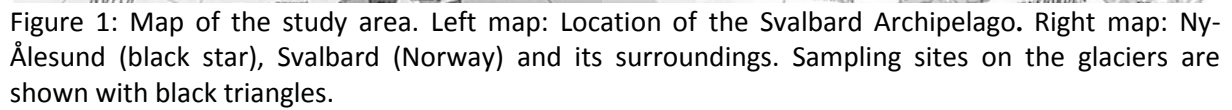
Figure 2: Principal component analysis for the sampling period. Chemical data ($\mu\text{mol.L}^{-1}$ or ng.L^{-1} for Hg species) were log-transformed prior to analysis. The data set covers the entire sampling period (16th April- June 8th). Abbreviations: Glut=glutaric acid, MSA=methanesulfonic acid, Ox=oxalic acid, For=formate, F=fluoride, Ace.Glyc=acetate-glycolate, BioHg=bioavailable Hg, THg=total Hg, MeHg=monomethylmercury, DHg=dissolved total Hg

Figure 3: Chemical profiles over time for organics (MSA, glutaric acid, oxalic acid) and different mercury species. Organic concentrations are expressed in $\mu\text{mol.L}^{-1}$, total mercury (THg) and bioavailable mercury (BioHg) are expressed in ng.L^{-1} . Monomethylmercury (MMHg) concentrations are expressed in pg.L^{-1} . Full squares represent surface samples, open squares represent basal samples and crosses are meltwater samples. Surface samples for MMHg and HgT are presented on a log-scale. All analyses were carried out in duplicate or triplicate and standard error was less than 10%.

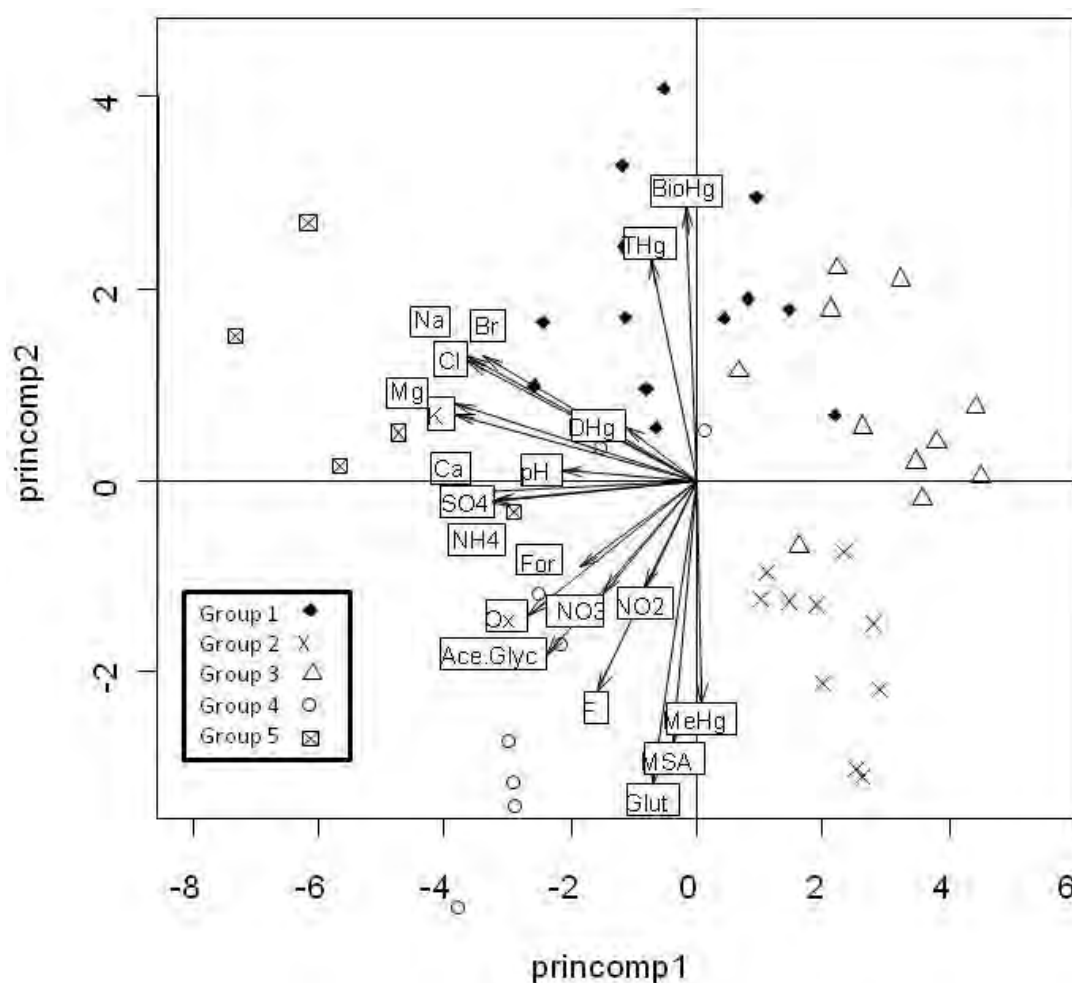
Figure 4: Meltwater elution curves for major ions and different mercury species over time. Ion concentrations are expressed in $\mu\text{mol.L}^{-1}$, total (THg), dissolved total (DHg) and bioavailable (BioHg) mercury concentrations are expressed in ng.L^{-1} . Monomethylmercury (MMHg) concentrations are in pg.L^{-1} . Analyses were carried out in duplicate or triplicate and standard error was less than 10%.

Figure 5: Snowpit total mercury (THg) and monomethylmercury (MMHg) profiles for Holtedahlfonna (sample date 30/04/2008) and Kongsvegen (sample date 19/05/2008) glaciers.

Figure 6: Sulfur cycle (modified from Bentley and Chasteen (2004)). The pathways represented here focus on biogenic transformations and the numbered pathways represent those discussed in the text. Other transformations occur but are not addressed in this paper. The pathways are: 1) DMSP-lyase. 2) Demethylation. 3) MMPA demethylation. 4) Thiol transmethylation. 5) Thiol transmethylation. The star symbol represents reactions where BioHg could potentially be methylated through methyltransfer reactions.



538
539



540
541 Figure 2: Principal component analysis for the sampling period. Chemical data ($\mu\text{mol.L}^{-1}$ or ng.L^{-1} for
542 Hg species) were log-transformed prior to analysis. The data set covers the entire sampling period
543 (16th April- June 8th). Abbreviations: Glut=glutaric acid, MSA=methanesulfonic acid, Ox=oxalic acid,
544 For=formate, F=fluoride, Ace.Glyc=acetate-glycolate, BioHg=bioavailable Hg, THg=total Hg,
545 MeHg=methylmercury, DHg=dissolved total Hg
546

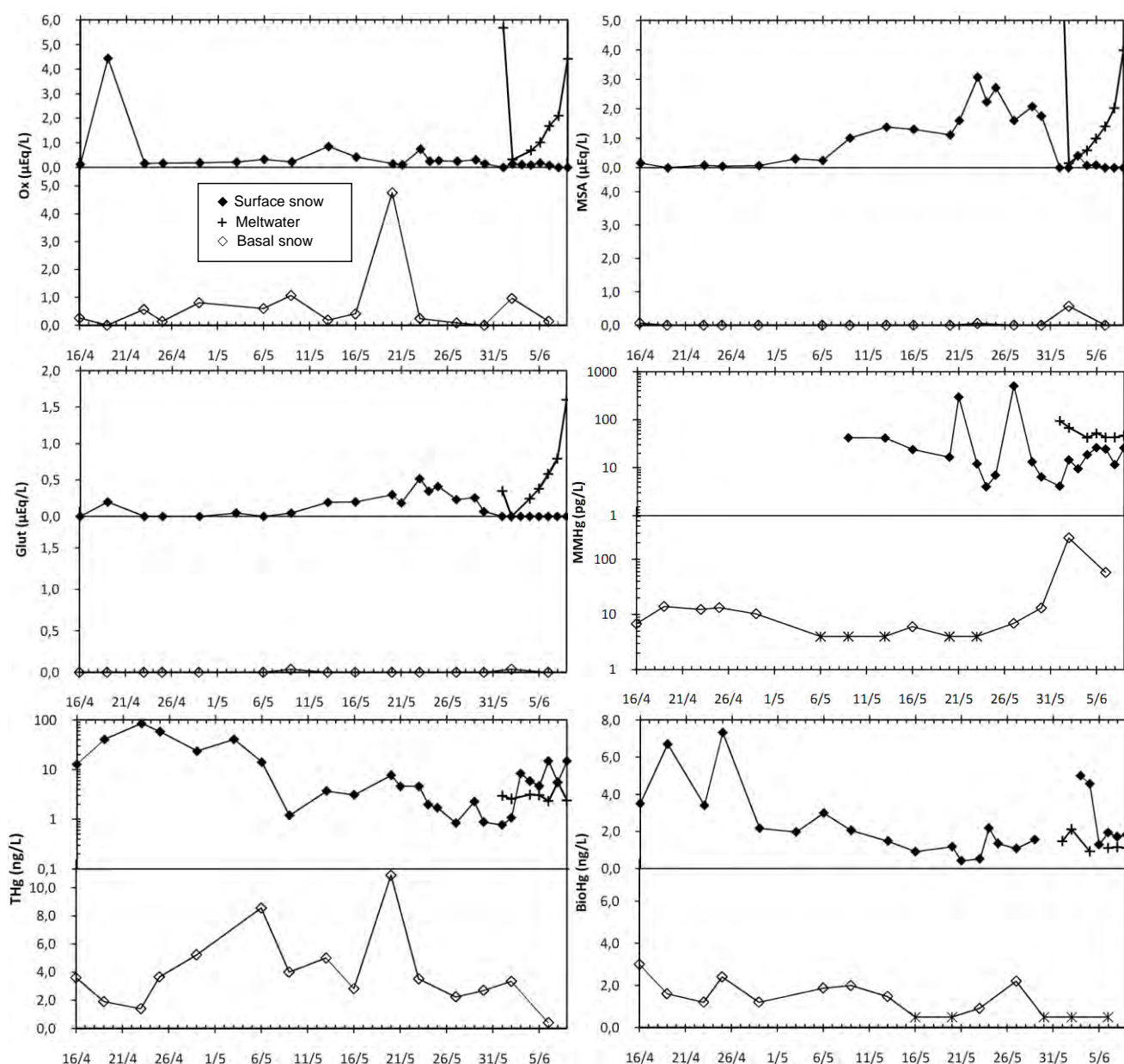


Figure 3: Chemical profiles over time for organics (MSA, glutaric acid, oxalic acid) and different mercury species. Organic concentrations are expressed in $\mu\text{mol.L}^{-1}$, total mercury (THg) and bioavailable mercury (BioHg) are expressed in ng.L^{-1} . Monomethylmercury (MMHg) concentrations are expressed in pg.L^{-1} . Full squares represent surface samples, open squares represent basal samples and crosses are meltwater samples. Surface samples for MMHg and HgT are presented on a log-scale. All analyses were carried out in duplicate or triplicate and standard error was less than 10%.

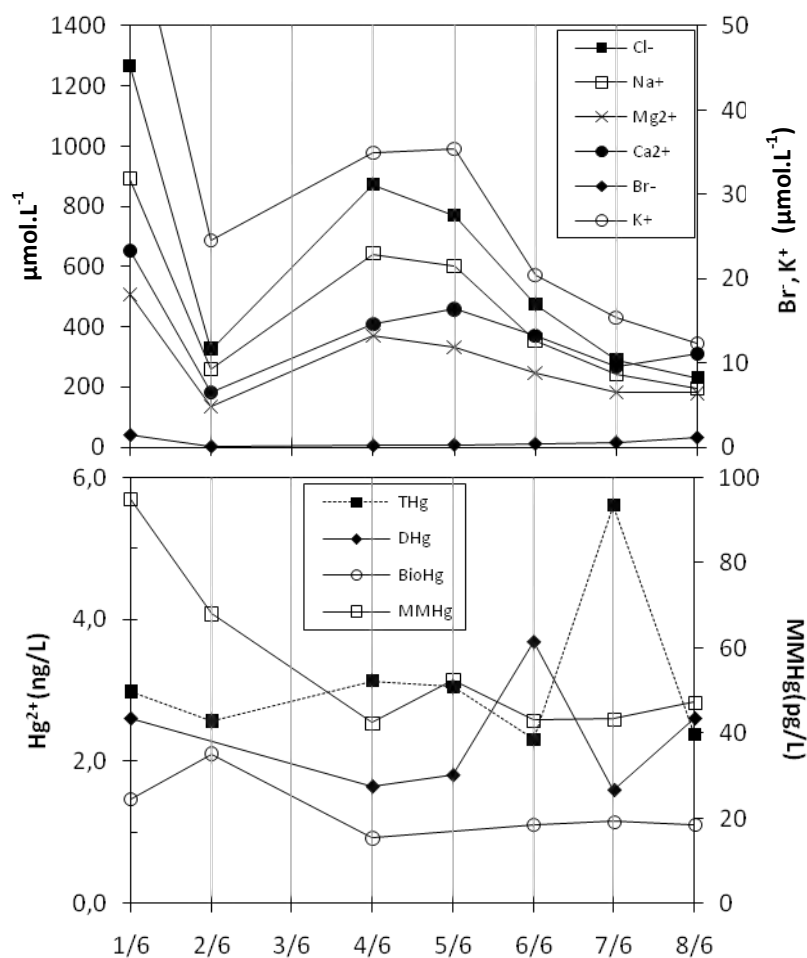
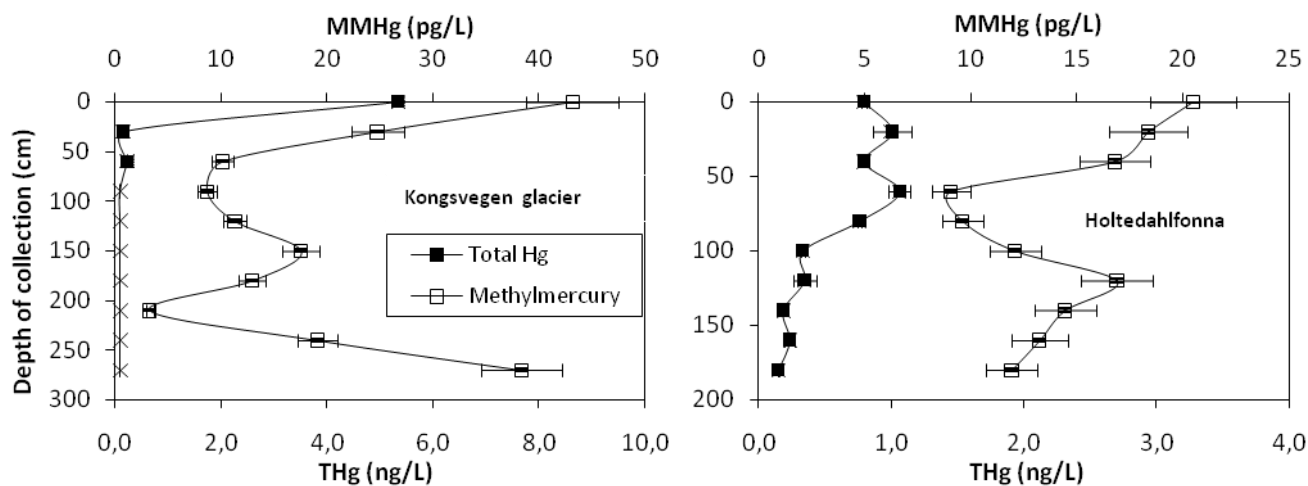


Figure 4: Meltwater elution curves for major ions and different mercury species over time. Ion concentrations are expressed in $\mu\text{mol.L}^{-1}$, total (THg), dissolved total (DHg) and bioavailable (BioHg) mercury concentrations are expressed in ng.L^{-1} . Methylmercury (MMHg) concentrations are in pg.L^{-1} . Analyses were carried out in duplicate or triplicate and standard error was less than 10%.

568



569

570 Figure 5: Snowpit total mercury (THg) and monomethylmercury (MMHg) profiles for Holtedahlfonna
571 (sample date 30/04/2008) and Kongsvegen (sample date 19/05/2008) glaciers. ▲

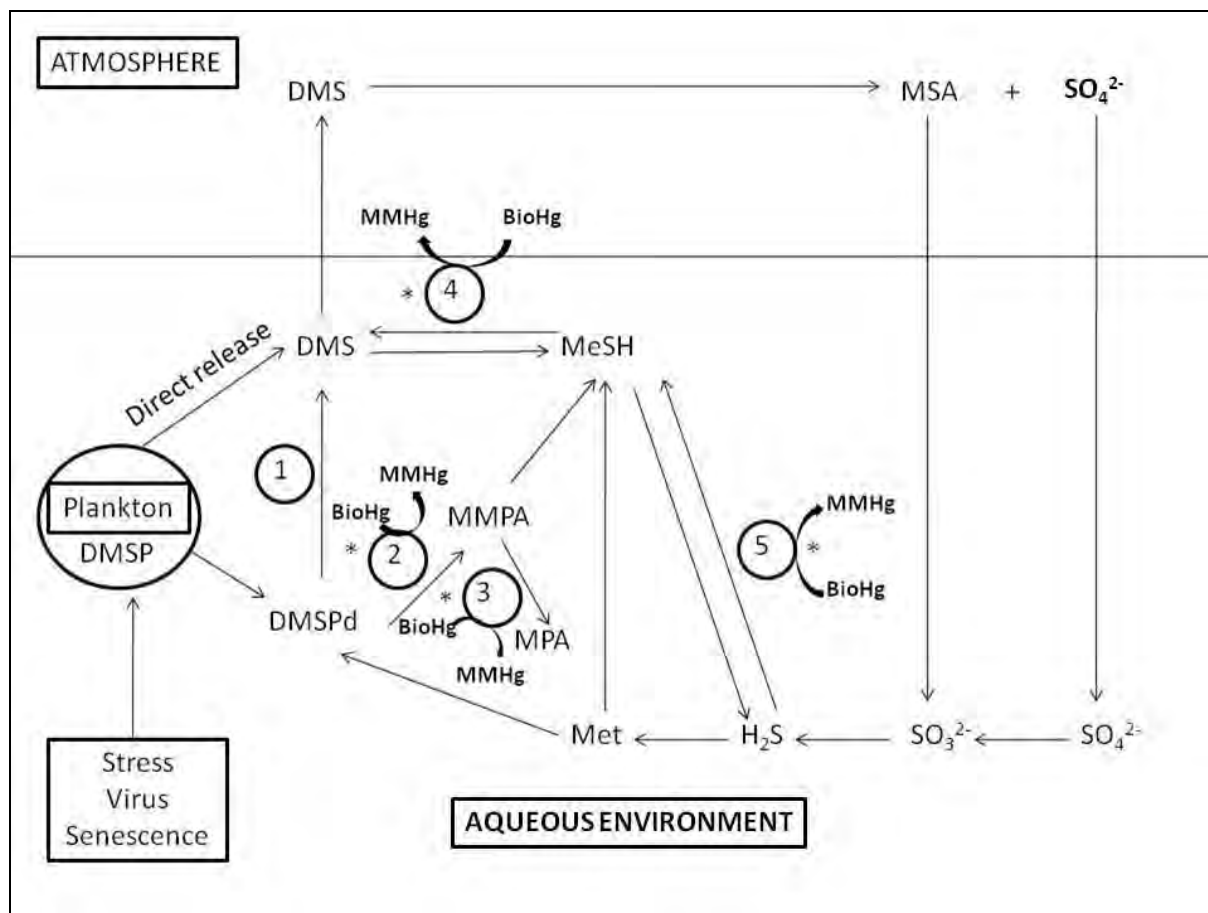
572

573

574

575

576
577



578

579 Figure 6: Sulfur cycle (modified from Bentley and Chasteen (2004)). The pathways represented here
580 focus on biogenic transformations and the numbered pathways represent those discussed in the
581 text. Other transformations occur, but are not addressed in this paper. The pathways are: 1) DMSP-
582 lyase. 2) Demethylation. 3) MMPA demethylation. 4) Thiol transmethylation. 5) Thiol
583 transmethylation. The star symbol represents reactions where BioHg could potentially be methylated
584 through methyltransfer reactions.

585
586

587

588

REFERENCES

- 589 AMAP, 2009. AMAP Assessment 2009: Human Health in the Arctic. Arctic Monitoring and Assessment
590 Programme (AMAP), Oslo, Norway.
- 591 Amato P., Hennebelle R., Magand O., Sancelme M., Delort A. M., Barbante C., Boutron C., and Ferrari
592 C. (2007) Bacterial characterization of the snow cover at Spitzberg, Svalbard. *FEMS Microbiol.*
593 *Ecol.* **59**, 255-264.
- 594 Ariya P. A., Khalizov A., and Gidas A. (2002) Reactions of gaseous mercury with atomic and molecular
595 halogens: Kinetics, product studies, and atmospheric implications. *J. Phys. Chem. A* **106**,
596 7310-7320.
- 597 Bales R. C., Davis R. E., and Williams M. W. (1993) Tracer release in melting snow: diurnal and
598 seasonal patterns. *Hydrolog. Process.* **7**, 389-401.
- 599 Barkay T., Gillman M., and Turner R. R. (1997) Effects of dissolved organic carbon and salinity on
600 bioavailability of mercury. *Appl. Environ. Microbiol.* **63**, 4267-71.
- 601 Barkay T. and Poulain A. J. (2007) Mercury (micro)biogeochemistry in polar environments. *FEMS*
602 *Microbiol. Ecol.* **59**, 232-41.
- 603 Bentley R. and Chasteen T. G. (2004) Environmental VOSCs--formation and degradation of dimethyl
604 sulfide, methanethiol and related materials. *Chemosphere* **55**, 291-317.
- 605 Berman M., Chase T., Jr., and Bartha R. (1990) Carbon Flow in Mercury Biomethylation by
606 *Desulfovibrio desulfuricans*. *Appl. Environ. Microbiol.* **56**, 298-300.
- 607 Brooks S., Lindberg S., Southworth G., and Arimoto R. (2008) Springtime atmospheric mercury
608 speciation in the McMurdo, Antarctica coastal region. *Atmos. Environ.* **42**, 2885-2893.
- 609 Campbell L. M., Norstrom R. J., Hobson K. A., Muir D. C. G., Backus S., and Fisk A. T. (2005) Mercury
610 and other trace elements in a pelagic Arctic marine food web (Northwater Polynya, Baffin
611 Bay). *Sci. Total Environ.* **351**, 247-263.
- 612 Celo V., Lean D. R., and Scott S. L. (2006) Abiotic methylation of mercury in the aquatic environment.
613 *Sci. Total Environ.* **368**, 126-37.
- 614 Choi S. C., Chase Jr. T., and Bartha R. (1994) Enzymatic catalysis of mercury methylation by
615 *Desulfovibrio desulfuricans* LS. . *Appl. Environ. Microbiol.* **60** 1342-1346.
- 616 Christner B. C. (2002) Incorporation of DNA and protein precursors into macromolecules by bacteria
617 at -15 degrees C. *Appl. Environ. Microbiol.* **68**, 6435-8.
- 618 Colbeck S. C. (1981) A simulation of the enrichment of atmospheric pollutants in snow cover runoff.
619 *Water Resour. Res.* **17** 1383-1388.
- 620 Colbeck S. C. (1989) Air movement in snow due to windpumping. *J Glaciol* **35**, 209-213.
- 621 Compeau G. C. and Bartha R. (1985) Sulfate reducing bacteria: principal methylators of mercury in
622 anoxic estuarine sediment. *Appl. Environ. Microbiol.* **50**, 498-502.
- 623 Constant P., Poissant L., Villemur R., Yumvihoze E., and Lean D. (2007) Fate of inorganic mercury and
624 methyl mercury within the snow cover in the low arctic tundra on the shore of Hudson Bay
625 (Québec, Canada). *J. Geophys. Res.* **112**.
- 626 Cossa D., Averty B., and Pirrone N. (2009) The origin of methylmercury in open Mediterranean
627 waters. *Limnol. Oceanogr.* **54**, 837-844.
- 628 Daly G. L. and Wania F. (2004) Simulating the Influence of Snow on the Fate of Organic Compounds.
629 *Environ. Sci. Technol.* **38**, 4176-4186.
- 630 Davies T. D., Vincent C. E., and Brimblecombe P. (1982) Preferential elution of strong acids from a
631 Norwegian ice cap. *Nature* **300**, 161-163.
- 632 Dommergue A., Ferrari C. P., Poissant L., Gauchard P. A., and Boutron C. F. (2003) Diurnal cycles of
633 gaseous mercury within the snowpack at Kuujuaupik/Whapmagoostui, Quebec, Canada.
634 *Environ. Sci. Technol.* **37**, 3289-97.

- Dommergue A., Larose C., Faïn X., Clarisse O., Foucher D., Hintelmann H., Schneider D., and Ferrari C. P. (2010) Deposition of mercury species in the Ny-Ålesund area (79°N) and their transfer during snowmelt. *Environ. Sci. Technol.* **44**, 901-907
- Douglas T. A. and Sturm M. (2004) Arctic haze, mercury and the chemical composition of snow across northwestern Alaska. *Atmos. Environ.* **38**, 805-820.
- Edwards A. C., Scalenghe R., and Freppaz M. (2007) Changes in the seasonal snow cover of alpine regions and its effect on soil processes: A review. *Quatern. Int.* **162–163** 172–181.
- Eichler A., Schwikowski M., and Gäggeler H. W. (2001) Meltwater induced relocation of chemical species in Alpine firn. *Tellus* **53B**, 192–203.
- Ferrari C. P., Moreau A. L., and Boutron C. F. (2000) Clean conditions for the determination of ultra-low levels of mercury in ice and snow samples. *Fresen. J. Anal. Chem.* **366**, 433–437.
- Fitzgerald W. F., Lamborg C. H., and Hammerschmidt C. R. (2007) Marine Biogeochemical Cycling of Mercury. *Chem. Rev.* **107**, 641-662.
- Fleming E. J., Mack E. E., Green P. G., and Nelson D. C. (2006) Mercury Methylation from Unexpected Sources: Molybdate-Inhibited Freshwater Sediments and an Iron-Reducing Bacterium. *Appl. Environ. Microbiol.* **72**, 457-464.
- Gardfeldt K., Munthe J., Stromberg D., and Lindqvist O. (2003) A kinetic study on the abiotic methylation of divalent mercury in the aqueous phase. *Sci. Total Environ.* **304**, 127-136.
- Goto-Azuma K., Nakawo M., Han J., Watanabe O., and Azuma N. (1994) Melt-induced relocation of ions in glaciers and in a seasonal snowpack *IAHS Publ.* **223** 287–298.
- Grannas A. M., Bausch A. R., and Mahanna K. M. (2007a) Enhanced aqueous photochemical reaction rates after freezing. *J. Phys. Chem. A* **111**, 11043-9.
- Grannas A. M., Jones A. E., Dibb J., Ammann M., Anastasio C., Beine H. J., Bergin M., Bottenheim J., Boxe C. S., Carver G., Chen G., Crawford J. H., Dominé F., Frey M. M., Guzman M. I., Heard D. E., Helmig D., Hoffmann M. R., Honrath R. E., Huey L. G., Hutterli M., Jacobi H. W., Klan P., Lefer B., McConnell J., Plane J., Sander R., Savarino J., Shepson P. B., Simpson W. R., Sodeau J. R., von Glasow R., Weller R., Wolff E. W., and Zhu T. (2007b) An overview of snow photochemistry: evidence, mechanisms and impacts. *Atmos. Chem. Phys.* **7**, 4329-4373.
- Hall B., Bloom N. S., and Munthe J. (1995) An experimental study of two potential methylation agents of mercury in the atmosphere: CH₃I and DMS. *Water Air Soil Pollut.* **80**, 337-341.
- Hammerschmidt C. R., Lamborg C. H., and Fitzgerald W. F. (2007) Aqueous phase methylation as a potential source of methylmercury in wet deposition. *Atmos. Environ.* **41**, 1663-1668.
- Hinkler J., Hansen B. U., Tamstorf M. P., Sigsgaard C., and Petersen D. (2008) Snow and Snow-Cover in Central Northeast Greenland. *Adv. Ecol. Res.* **40**, 175-195.
- Hodgkins R., Tranter, M., and Dowdeswell, J. A. (1998) The hydrochemistry of runoff from a 'coldbased' glacier in the High Arctic (Scott Turnerbreen, Svalbard) *Hydrol. Process.* **12**, 87–103.
- Johannessen M. and Henriksen A. (1978) Chemistry of snow melt water: changes in concentration during melting *Water Resour. Res.* **14**, 615-619.
- Johnson K. P., Blum J. D., Keeler G. J., and Douglas T. A. (2008) Investigation of the deposition and emission of mercury in arctic snow during an atmospheric mercury depletion event. *J. Geophys. Res.* **113**, doi:10.1029/2008JD009893.
- Jones H. G. (1999) The ecology of snow-covered systems: a brief overview of nutrient cycling and life in the cold. *Hydrol Process* **13**, 2135–2147.
- Kawamura K. and Ikushima K. (1993) Seasonal changes in the distribution of dicarboxylic acids in the urban atmosphere. *Envir. Sci. Technol.* **27**, 2227-2235.
- Kawamura K. and Kasukabe H. (1996) Sources and reaction pathways of dicarboxylic acids, ketoacids and dicarbonyls in Arctic aerosols: one year of observations. *Atmos. Environ.* **30**, 1709-1722.
- Kerin E. J., Gilmour C. C., Roden E., Suzuki M. T., Coates J. D., and Mason R. P. (2006) Mercury Methylation by Dissimilatory Iron-Reducing Bacteria. *Appl. Environ. Microbiol.* **72**, 7919-7921.

- 685 Kiene R. P., Linn L. J., and Bruton J. A. (2000) New and important roles for DMSP in marine microbial
686 communities. *J. Sea Res.* **43**, 209-224.
- 687 Kirk J. L., St. Louis V. L., Hintelmann H., Lehnher I., Else B., and Poissant L. (2008) Methylated
688 Mercury Species in Marine Waters of the Canadian High and Sub Arctic. *Environ. Sci. Technol.*
689 **42**, 8367-8373.
- 690 Kirk J. L., St. Louis V. L., and Sharp M. J. (2006) Rapid Reduction and Reemission of Mercury Deposited
691 into Snowpacks during Atmospheric Mercury Depletion Events at Churchill, Manitoba,
692 Canada. *Environ. Sci. Technol.* **40**, 7590-7596.
- 693 Kuhn M. (1987) Micro-meteorological conditions for snow melt *J Glaciol* **33**, 24-26.
- 694 Kuhn M. (2001) The nutrient cycle through snow and ice, a review. *Aqua. Sci.* **63**, 150-167.
- 695 Lalonde J. D., Poulain A. J., and Amyot M. (2002) The role of mercury redox reactions in snow on
696 snow-to-air mercury transfer. *Environ. Sci. Technol.* **36**, 174-178.
- 697 ~~Larose C., Dommergue A., Ferrari C., Maruszczak N., Coves J., and Schneider D. (2010) Detection of~~
698 ~~bioavailable Hg deposited in Polar regions. *The ISME Journal* submitted.~~
- 699 Leck C. and Persson C. (1996) The central Arctic Ocean as a source of dimethyl sulfide - Seasonal
700 variability in relation to biological activity *Tellus* **48B**, 156-177.
- 701 Legrand M., Preunkert S., Oliveira T., Pio C. A., Hammer S., Gelencsér A., Kasper-Giebl A., and Laj P.
702 (2007) Origin of C2-C5 dicarboxylic acids in the European atmosphere inferred from year-
703 round aerosol study conducted at a west-east transect. *J. Geophys. Res.* **112**, D23S07,
704 doi:10.1029/2006JD008019.
- 705 Lei Y. D., D. Y., and Wania F. (2004) Is rain or snow a more efficient scavenger of organic chemicals?
706 *Atmos. Environ.* **38**, 3557-3571.
- 707 Lindberg S. E., Brooks S., Lin C. J., Scott K., Meyers T., Chambers L., Landis M., and Stevens R. (2001)
708 Formation of Reactive Gaseous Mercury in the Arctic: Evidence of Oxidation of Hg⁰ to Gas-
709 Phase Hg-II Compounds after Arctic Sunrise. *Water Air Soil Poll. Focus* **1**, 295-302.
- 710 Lindberg S. E., Brooks S., Lin C. J., Scott K. J., Landis M. S., Stevens R. K., Goodsite M., and Richter A.
711 (2002) Dynamic Oxidation of Gaseous Mercury in the Arctic Troposphere at Polar Sunrise.
712 *Environ. Sci. Technol.* **36**, 1245-256.
- 713 Loseto L. L., Lean D. R. S., and Siciliano S. D. (2004) Snowmelt Sources of Methylmercury to High
714 Arctic Ecosystems. *Environ. Sci. Technol.* **38**, 3004-3010.
- 715 Lu J. Y., Schroeder W. H., Barrie L. A., Steffen A., Welch H. E., Martin K., Lockhart L., Hunt R. V., Boila
716 G., and Richter A. (2001) Magnification of atmospheric mercury deposition to polar regions in
717 springtime: the link to tropospheric ozone depletion chemistry. *Geophys. Res. Lett.* **28**, 3219-
718 3222.
- 719 Lyons W. B., Welch K. A., Fountain A. G., Dana G. L., Vaughn B. H., and McKnight D. M. (2003) Surface
720 glaciochemistry of Taylor Valley, southern Victoria Land, Antarctica, and its relation to stream
721 chemistry. *Hydrolog. Process.* **17** 115-130.
- 722 Meyer T., Lei Y. D., and Wania F. (2006) Measuring the release of organic contaminants from melting
723 snow under controlled conditions. *Environ. Sci. Technol.* **40**, 3320-3326.
- 724 Meyer T. and Wania F. (2008) Organic contaminant amplification during snowmelt. *Water Res.* **42**,
725 1847-1865.
- 726 Monperrus M., Tessier E., Amouroux D., Leynaert A., Huonnic P., and Donard O. F. X. (2007) Mercury
727 methylation, demethylation and reduction rates in coastal and marine surface waters of the
728 Mediterranean Sea. *Mar. Chem.* **107**, 49-63.
- 729 Narcy F., Gasparini S., Falk-Petersen S., and Mayzaud P. (2009) Seasonal and individual variability of
730 lipid reserves in *Oithona similis* (Cyclopoida) in an Arctic fjord. *Polar Biol.* **32**, 233-242.
- 731 Niki H., Maker P. D., Savage C. M., and Breitenbach L. P. (1983a) A long-path Fourier transform
732 infrared study of the kinetics and mechanism for the hydroxyl radical-initiated oxidation of
733 dimethylmercury. *J. Phys. Chem.* **87**, 4978 - 4981.

- Niki H., Maker P. S., Savage C. M., and Breitenbach L. P. (1983b) A Fourier-transform infrared study of the kinetics and mechanism of the reaction of atomic chlorine with dimethylmercury. *J. Phys. Chem.* **87**, 3722-3724.
- Poulain A. J., Lalonde J. D., Amyot M., Shead J. A., Raofie F., and Ariya P. A. (2004) Redox transformations of mercury in an Arctic snowpack at springtime. *Atmos. Environ.* **38**, 6763-6774.
- Poulain A. J., Ni Chadhain S. M., Ariya P. A., Amyot M., Garcia E., Campbell P. G. C., Zylstra G. J., and Barkay T. (2007) Potential for mercury reduction by microbes in the high arctic. *Appl. Environ. Microbiol.* **73**, 2230-2238.
- Reisch C. R., Moran M. A., and Whitman W. B. (2008) Dimethylsulfoniopropionate-dependent demethylase (DmdA) from *Pelagibacter ubique* and *Silicibacter pomeroyi*. *J. Bacteriol.* **190**, 8018-24.
- Rontani J.-F. (2001) Visible light-dependent degradation of lipidic phytoplanktonic components during senescence: a review. *Phytochemistry* **58**, 187-202.
- Schroeder W. H., Anlauf K. G., Barrie L. A., Lu J. Y., Steffen A., Schneeberger D. R., and Berg T. (1998) Arctic springtime depletion of mercury. *Nature* **394**, 331-332.
- Scott K. J. (2001) Bioavailable mercury in arctic snow determined by a light-emitting mer-lux bioreporter. *Arctic* **54**, 92-95.
- Siciliano S. D., O'Driscoll N. J., Tordon R., Hill J., Beauchamp S., and Lean D. R. S. (2005) Abiotic production of methylmercury by solar radiation. *Environ. Sci. Technol.* **39**, 1071-1077.
- St. Louis V. L., Hintelmann H., Graydon J. A., Kirk J. L., Barker J., Dimock B., Sharp M. J., and Lehnher I. (2007) Methylated mercury species in Canadian high arctic marine surface waters and snowpacks. *Environ. Sci. Technol.* **41**, 6433-6441.
- St. Louis V. L., Sharp M. J., Steffen A., May A., Barker J., Kirk J. L., Kelly D. J. A., Arnott S. E., Keatley B., and Smol J. P. (2005) Some sources and sinks of monomethyl and inorganic mercury on Ellesmere island in the Canadian high arctic. *Environ. Sci. Technol.* **39**, 2686-2701.
- Stoichev T., Rodriguez Martin-Doimeadios R. C., Tessier E., Amouroux D., and Donard O. F. (2004) Improvement of analytical performances for mercury speciation by on-line derivatization, cryofocussing and atomic fluorescence spectrometry. *Talanta* **62**, 433-8.
- Sunderland E. M., Krabbenhoft D. P., Moreau J. W., Strode S. A., and Landing W. M. (2009) Mercury sources, distribution, and bioavailability in the North Pacific Ocean: Insights from data and models. *Global Biogeochem. Cycles* **23**.
- Tranter M., Brimblecombe P., Davies T. D., Vincent C. E., Abrahams P. W., and Blackwood I. (1986) A composition of snowfall, snowpack and meltwater in the Scottish Highlands—evidence for preferential elution *Atmos. Environ.* **20**, 517-525.
- Tseng C. M., Garraud H., Amouroux D., Donard O. F., and de Diego A. (1998) Open focused microwave-assisted sample preparation for rapid total and mercury species determination in environmental solid samples. *J. Autom. Chem.* **20**, 99-108.
- Wagemann R., Trebacz E., Boila G., and Lockhart W. L. (1998) Methylmercury and total mercury in tissues of arctic marine mammals. *Sci. Total Environ.* **218**, 19-31.
- Weber J. H. (1993) Review of possible paths for abiotic methylation of mercury(II) in the aquatic environment. *Chemosphere* **26**, 2063-2077.
- Williams M. W., Seibold C., and Chowanski K. (2009) Storage and release of solutes from a subalpine seasonal snowpack: soil and stream water response, Niwot Ridge, Colorado. *Biogeochemistry* **95**, 77-94.